NASA TECHNICAL REPORT

NASA TR R-242

NASA TR R-242

ANALYTICAL STUDY OF DIFFUSION-CONTROLLED CHAR OXIDATION AND ITS EFFECT ON STEADY-STATE ABLATION OF PLASTIC MATERIALS

by Gerald D. Walberg

Langley Research Center
Langley Station, Hampton, Va.

NATIONAL AERONAUTICS AND SPACE ADMINISTRATION • WASHINGTON, D. C. • JULY 1966

, 0166

Dist. List ( )

	TO:	DISPOSITION: PLASTEC	DISPOSITION: Destroy
( )	Pebly	( )	( )
( )	Baldanza	( )	( )
( )	Beach	( )	( )
( )	Landrock	( )	( )
( )	Molzon	( )	( )
(X)	Shibley	(X)	( )
( )	Titus	( )	( )
( )	Anzalone	( )	( )

COMMENTS: Vendor - received
one PTEC No.

Col.

NASA TR R-242

ANALYTICAL STUDY OF DIFFUSION-CONTROLLED CHAR OXIDATION AND ITS EFFECT ON STEADY-STATE ABLATION OF PLASTIC MATERIALS

By Gerald D. Walberg

Langley Research Center
Langley Station, Hampton, Va.

NATIONAL AERONAUTICS AND SPACE ADMINISTRATION

For sale by the Clearinghouse for Federal Scientific and Technical Information
Springfield, Virginia 22151 – Price $2.00

ANALYTICAL STUDY OF DIFFUSION-CONTROLLED CHAR OXIDATION AND ITS EFFECT ON STEADY-STATE ABLATION OF PLASTIC MATERIALS

By Gerald D. Walberg
Langley Research Center

SUMMARY

An analysis of diffusion-controlled char oxidation has been carried out and differs from previous analyses in one important respect: previous investigators have assumed that only the carbon present in the char would react, but the present analysis has shown that the carbon present in both the char and the pyrolysis gases (i.e., all the carbon originally present in the virgin plastic) reacts and that the reaction rate is determined by the rate at which oxygen can be supplied by diffusion through the boundary layer plus pyrolysis of the plastic. Because of this fact, the char oxidation rate, the steady-state ablation rate, the boundary-layer composition at the char surface, and the heat released by chemical reactions were found to be dependent on the composition of the virgin plastic and the pyrolysis gases.

For a given flow environment, the char oxidation rate and the steady-state pyrolysis rate were found to increase as the hydrogen, nitrogen, and oxygen contents of the virgin plastic increased and to decrease as the carbon content of the virgin plastic increased. It was found that the heat released by both gas phase and heterogeneous reactions can be accounted for by an "effective enthalpy potential" which is a function of the stream oxygen mass fraction and the compositions of the virgin plastic and the pyrolysis gases. Particularly high heat releases are predicted for polymers which contain nearly equal numbers of carbon and oxygen atoms and produce pyrolysis gases containing large quantities of C_2H_2 and C_2H_4.

INTRODUCTION

Since the efficiency of a charring ablator is determined to a large extent by the char removal rate, an understanding of char removal mechanisms is essential for the prediction of the performance of a charring ablator. For the steady-state ablation case, the linear rate of pyrolysis is equal to the char removal rate; hence, the virgin plastic pyrolysis rate is known if the char removal rate can be determined.

When the char layer under consideration possesses adequate structural strength so that mechanical failure (removal by aerodynamic shear, spallation, etc.) does not occur, the char removal rate is determined by the rate of chemical reaction between the char, the gaseous pyrolysis products, and the chemical species present in the boundary layer. Since an ablator which loses large amounts of char due to mechanical failure is not suitable for use on reentry heat shields, it is not unreasonable to expect that chemical reactions will be the primary char removal mechanism during most reentries.

The maximum rate at which char oxidation can proceed is ultimately determined by the rate at which fresh supplies of oxygen can be transported to the char surface. When a laminar boundary layer exists over the char surface, the transport mechanism of interest is molecular diffusion and this maximum rate is referred to as the diffusion-controlled oxidation rate. Since carbonaceous materials possess extremely high intrinsic chemical reactivities at temperatures above 3000° R (1667° K) (refs. 1 and 2), the char-layer oxidation is generally assumed to be diffusion controlled under most reentry conditions. (See refs. 1 to 5.)

In the present report, an analytical study of the diffusion-controlled oxidation of an ablative char layer is presented and, within a range of pressure and temperature which is typical of stagnation-point conditions during orbital reentry, an approximate closed-form solution is obtained. Although this solution is based on a number of simplifying assumptions, it is believed to be a sound conceptual picture of the diffusion-controlled oxidation process which demonstrates the role of pyrolysis gases in determining the oxidation rate (and hence the steady-state pyrolysis rate) and provides a relation between the original chemical composition and the cold-wall effective heat of ablation of a charring ablator.

SYMBOLS

All dimensional quantities are presented in terms of both U.S. Customary Units and the International (SI) System of Units. (See ref. 6.)

A,B,C,D	stoichiometric coefficients per mole of boundary-layer gas mixture (see eq. (100))
a,b,. . .,o	equilibrium coefficients (see eqs. (71) to (85))
c_p	specific heat of boundary-layer gas mixture, British thermal units per pound-$^{\circ}$R (joules per kilogram-$^{\circ}$K)

D	coefficient of diffusion, feet^2 per second (meters^2 per second)
f	mass of char produced by decomposition of unit mass of virgin plastic
H	stream enthalpy, British thermal units per pound (joules per kilogram)
ΔH	enthalpy potential across boundary layer, $H_e - H_w$, British thermal units per pound (joules per kilogram)
ΔH_R	overall heat of reaction, British thermal units per mole of carbon (solid) (joules per mole of carbon (solid)) (see eqs. (113) and (116))
$\Delta H_{f,i}$	heat of formation of species i, British thermal units per mole of i (joules per mole of i)
h	convective heat-transfer coefficient, pounds per foot^2-second (kilograms per meter^2-second)
h_m	mass-transfer coefficient, pounds per foot^2-second (kilograms per meter^2-second)
K_i	mass fraction of species i, mass of i per unit mass of gas mixture
$\tilde{K}_i$	elemental mass fraction, mass of chemical element i (no matter what chemical form it may appear in) per unit mass of gas mixture
$\hat{K}_i$	mass of species i per unit mass of gases injected into boundary layer
$K_{p,(n)}$	equilibrium constant (expressed in terms of partial pressures) for reaction presented in equation (n)
k	thermal conductivity of boundary-layer gas mixture, British thermal units per foot-second-$^\circ$F (joules per meter-second-$^\circ$K)
l	exponent in transpiration cooling expression (see eqs. (125) and (127))
$\overline{M}$	molecular weight of gas mixture at char surface
$\hat{M}$	average molecular weight of gases injected into boundary layer

M_i	molecular weight of species i
$\dot{m}$	mass rate of oxidation or ablation, pounds per foot^2-second (kilograms per meter^2-second)
m_C	mass of carbon per unit mass of virgin plastic
m_H	mass of hydrogen per unit mass of virgin plastic
m_N	mass of nitrogen per unit mass of virgin plastic
m_O	mass of oxygen per unit mass of virgin plastic
N_A	Avogadro's number
N_{Le}	Lewis number, $\frac{\rho D_{12} c_p}{k}$
n_{ik}	number of moles of species i per mole of species k (see eq. (23))
p	pressure, pounds per foot^2 or atmospheres (newtons per meter^2)
p_i	partial pressure of species i, pounds per foot^2 (newtons per meter^2)
Q^*	thermochemical heat of ablation, British thermal units per pound (joules per kilogram) (see eq. (142))
Q_{eff}	cold-wall effective heat of ablation, $\frac{q_{cw}^{\ o}}{\dot{m}_{vp}}$, British thermal units per pound (joules per kilogram)
q	convective aerodynamic heat flux, British thermal units per foot^2-second (joules per meter^2-second)
q_{cw}	cold-wall aerodynamic heat flux, British thermal units per foot^2-second (joules per meter^2-second)
q_{net}	net heat flux to surface of ablator, used in defining Q^*, British thermal units per foot^2-second (joules per meter^2-second) (see eq. (142))

q_t	heat flux due to both convection and chemical reactions, British thermal units per foot^2-second (joules per meter^2-second)
r	nose radius of hemispherical body, feet (meters)
T	temperature, ^{o}R (^{o}K)
v	boundary-layer velocity normal to char surface, feet per second (meters per second)
W	ratio of diffusive oxygen flux to char oxidation rate, defined by equation (95)
X_i	mole fraction of species i, moles of i per mole of gas mixture
$\bar{X}_i$	moles of species i per mole of pyrolysis gas
y	distance normal to char surface, positive when directed away from char, feet (meters)
η	transpiration cooling factor (see eq. (120))
λ	ratio of virgin plastic pyrolysis rate to char oxidation rate (see eq. (7))
ρ	boundary-layer density, pounds per foot^3 (kilograms per meter^3)
σ,τ,ν,φ	indices in empirical polymer formulas, indicating the respective number of carbon, hydrogen, nitrogen, and oxygen atoms in the plastic

Subscripts:

C,H,N,O	pertaining to carbon, hydrogen, nitrogen, and oxygen, respectively
c	pertaining to ablative char layer
ch	pertaining to or resulting from chemical reactions
e	evaluated at outer edge of boundary layer

i,j,k	pertaining to ith, jth, or kth chemical species or element
s	evaluated at stagnation conditions
vp	pertaining to virgin plastic
w	evaluated at char surface
12	denoting values for binary gas mixture

Superscripts:

o	evaluated for zero mass injection into boundary layer
*	steady-state solution

ANALYSIS

In this section, the governing equations and the assumptions used in the present analysis are stated, and the ranges of temperature and pressure within which an approximate closed-form solution is obtainable are identified. The distance y used in this analysis and the various zones and interfaces pertinent to the behavior of a charring ablator as analyzed herein are presented in figure 1. The virgin plastic is assumed to contain only nitrogen, oxygen, carbon, and hydrogen.

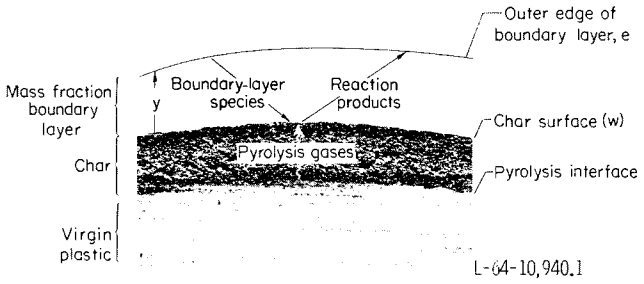

Figure 1.- Charring ablator showing zones and interfaces.

Governing Equations

Consider the decomposition of a hydrocarbon polymer according to the equation

$$C_\sigma H_\tau N_\nu O_\varphi \rightarrow \text{Pyrolysis gas} + C(s) \qquad (1)$$

At the char surface, mass conservation of the element nitrogen may be represented by the equation

$$-h_{m,N}\left(\tilde{K}_{N,e} - \tilde{K}_{N,w}\right) + \left(\tilde{K}_N \rho v\right)_w = \left(\frac{\nu M_N}{\sigma M_C + \tau M_H + \nu M_N + \varphi M_O}\right)\dot{m}_{vp} \quad (2)$$

Diffusion away from char surface

Convection away from char surface

Flow of pyrolysis gases from pyrolysis zone to char surface

where σ, τ, ν, and φ represent the relative number of atoms of carbon, hydrogen, nitrogen, and oxygen in the virgin plastic, and $h_{m,N}$ is the elemental mass-transfer coefficient for nitrogen, which is defined by the equation

$$\left(\rho D_N \frac{\partial \tilde{K}_N}{\partial y}\right)_w = h_{m,N}\left(\tilde{K}_{N,e} - \tilde{K}_{N,w}\right) \quad (3)$$

The quantity in parentheses on the right-hand side of equation (2) represents the mass of elemental nitrogen contained in the pyrolysis gases produced by decomposition of a unit mass of virgin plastic.

In order for equation (3) to be rigorously valid, all the species containing nitrogen must have nearly equal diffusion coefficients. Since subsequent equations will place similar requirements on the species containing oxygen, hydrogen, and carbon, the use of the diffusion coefficients D_N, D_O, D_H, and D_C implies that the diffusion coefficients of all the species are nearly equal - that is, the gas mixture is effectively binary. This binary mixture requirement is discussed in the section "Review of Assumptions." Equations similar to equation (2) may be written for oxygen, carbon, and hydrogen as follows:

$$-h_{m,O}\left(\tilde{K}_{O,e} - \tilde{K}_{O,w}\right) + \left(\tilde{K}_O \rho v\right)_w = \left(\frac{\varphi M_O}{\sigma M_C + \tau M_H + \nu M_N + \varphi M_O}\right)\dot{m}_{vp} \quad (4)$$

$$-h_{m,C}\left(\tilde{K}_{C,e} - \tilde{K}_{C,w}\right) + \left(\tilde{K}_C \rho v\right)_w = \left(\frac{\sigma M_C}{\sigma M_C + \tau M_H + \nu M_N + \varphi M_O} - f\right)\dot{m}_{vp} + \dot{m}_c \quad (5)$$

$$-h_{m,H}\left(\tilde{K}_{H,e} - \tilde{K}_{H,w}\right) + \left(\tilde{K}_H \rho v\right)_w = \left(\frac{\tau M_H}{\sigma M_C + \tau M_H + \nu M_N + \varphi M_O}\right)\dot{m}_{vp} \quad (6)$$

where f represents the mass of char produced by decomposition of a unit mass of virgin plastic. Now define λ as

$$\lambda = \frac{\dot{m}_{vp}}{\dot{m}_c} \quad (7)$$

and note that

$$(\rho v)_w = \dot{m}_c \left[1 + \lambda(1 - f)\right] \tag{8}$$

The respective masses of nitrogen, oxygen, carbon, and hydrogen per unit mass of virgin plastic can be expressed as

$$m_N = \frac{\nu M_N}{\sigma M_C + \tau M_H + \nu M_N + \varphi M_O} \tag{9}$$

$$m_O = \frac{\varphi M_O}{\sigma M_C + \tau M_H + \nu M_N + \varphi M_O} \tag{10}$$

$$m_C = \frac{\sigma M_C}{\sigma M_C + \tau M_H + \nu M_N + \varphi M_O} \tag{11}$$

$$m_H = \frac{\tau M_H}{\sigma M_C + \tau M_H + \nu M_N + \varphi M_O} \tag{12}$$

Substitution of equations (7) to (12) into equations (2), (4), (5), and (6) yields the following expressions for the elemental mass fractions at the char surface $\left(\text{by definition, } \tilde{K}_{C,e} = \tilde{K}_{H,e} = 0\right)$:

$$\tilde{K}_{N,w} = \frac{\tilde{K}_{N,e} h_{m,N} + m_N \lambda \dot{m}_c}{h_{m,N} + \left[1 + \lambda(1 - f)\right] \dot{m}_c} \tag{13}$$

$$\tilde{K}_{O,w} = \frac{\tilde{K}_{O,e} h_{m,O} + m_O \lambda \dot{m}_c}{h_{m,O} + \left[1 + \lambda(1 - f)\right] \dot{m}_c} \tag{14}$$

$$\tilde{K}_{C,w} = \frac{\left[1 + (m_C - f)\lambda\right] \dot{m}_c}{h_{m,C} + \left[1 + \lambda(1 - f)\right] \dot{m}_c} \tag{15}$$

$$\tilde{K}_{H,w} = \frac{m_H \lambda \dot{m}_c}{h_{m,H} + \left[1 + \lambda(1 - f)\right] \dot{m}_c} \tag{16}$$

Equations (13) to (16) are the governing equations for this study. These equations, however, cannot be solved unless the mass-transfer coefficients $h_{m,i}$ can be evaluated.

Evaluation of Mass-Transfer Coefficient

In this report, the mass-transfer coefficients $h_{m,i}$ are expressed in terms of the convective heat-transfer coefficient through the application of an analogy between the transfer of energy and mass in a laminar boundary layer. This analogy (with minor variations) is often used in treating the diffusion-controlled oxidation of graphite. (See refs. 2, 3, 7, 8, and 9.)

Lees in reference 9 shows that, for the case of a laminar, unit Lewis number, stagnation-point boundary layer, the ith elemental mass fraction and the total enthalpy are related by the following equation:

$$\frac{\tilde{K}_i - \tilde{K}_{i,w}}{\tilde{K}_{i,e} - \tilde{K}_{i,w}} = \frac{H_s - H_{s,w}}{H_{s,e} - H_{s,w}} \tag{17}$$

Hence

$$\frac{\partial \tilde{K}_i}{\partial y} = \frac{\tilde{K}_{i,e} - \tilde{K}_{i,w}}{H_{s,e} - H_{s,w}} \frac{\partial H_s}{\partial y} \tag{18}$$

and since

$$N_{Le} = \frac{\rho D_{12} c_p}{k} = 1 \tag{19}$$

it follows that

$$\rho D_{12} \frac{\partial \tilde{K}_i}{\partial y} = \left(\tilde{K}_{i,e} - \tilde{K}_{i,w}\right) N_{Le} \frac{q}{H_{s,e} - H_{s,w}} = \left(\tilde{K}_{i,e} - \tilde{K}_{i,w}\right) h \tag{20}$$

But the ith elemental mass-transfer coefficient is defined by the equation

$$\rho D_i \frac{\partial \tilde{K}_i}{\partial y} = \left(\tilde{K}_{i,e} - \tilde{K}_{i,w}\right) h_{m,i} \tag{21}$$

Hence, if the boundary-layer mixture is effectively binary,

$$h_{m,i} = h \tag{22}$$

This assumption is discussed in the section "Review of Assumptions."

Pyrolysis Gas Composition, Char Composition, Assumed Reactions, and Equilibrium Expressions

The elemental mass fractions $\tilde{K}_i$ which appear in equations (13) to (16) can be expressed in terms of the mole fractions of the various chemical species by the following equation:

$$\tilde{K}_i = \frac{M_i}{\bar{M}} \sum_k n_{ik} X_k \tag{23}$$

where

M_i atomic weight of elemental species i

$\bar{M}$ molecular weight of gas mixture

X_k mole fraction of kth chemical species in gas mixture

n_{ik} number of moles of i per mole of k

The chemical species which must be considered are determined by the reactions which take place between the pyrolysis gases, the boundary-layer species, and the char.

The elemental mass fractions $\tilde{K}_{i,w}$ are expressed in terms of the reactants and products under the assumption that chemical equilibrium (both heterogeneous and gas phase) exists at the char surface. The pyrolysis gases are assumed to be composed of N_2, H_2, NH_3, CO, CO_2, H_2O, C_2H_2, C_2H_4, and CH_4, and the char is assumed to be graphite.

The following chemical reactions are considered:

$$2NH_3 \rightleftharpoons 3H_2 + N_2 \tag{24}$$

$$CH_4 + 2O_2 \rightleftharpoons CO_2 + 2H_2O \tag{25}$$

$$C_2H_2 + \frac{5}{2} O_2 \rightleftharpoons 2CO_2 + H_2O \tag{26}$$

$$C_2H_4 + 2O_2 \rightleftharpoons 2CO + 2H_2O \tag{27}$$

$$\frac{1}{2}O_2 \rightleftharpoons O \tag{28}$$

$$\frac{1}{2}H_2 \rightleftharpoons H \tag{29}$$

$$\frac{1}{2}H_2 + \frac{1}{2}O_2 \rightleftharpoons OH \tag{30}$$

$$H_2 + \frac{1}{2}O_2 \rightleftharpoons H_2O \tag{31}$$

$$\frac{1}{2}N_2 \rightleftharpoons N \tag{32}$$

$$\frac{1}{2}N_2 + \frac{1}{2}O_2 \rightleftharpoons NO \tag{33}$$

$$C(s) \rightleftharpoons C(g) \tag{34}$$

$$C(s) + \frac{1}{2}O_2 \rightleftharpoons CO \tag{35}$$

$$C(s) + CO_2 \rightleftharpoons 2CO \tag{36}$$

$$C(s) + H_2O \rightleftharpoons H_2 + CO \tag{37}$$

$$C(s) + N \rightleftharpoons CN \tag{38}$$

$$C(s) + NH_3 \rightleftharpoons HCN + H_2 \tag{39}$$

The notation s or g indicates species in a solid or gaseous state, respectively. The equilibrium constants for reactions (eqs. (24) to (39)) may be written as follows:

$$K_{p,(24)} = \frac{p_{H_2}{}^3 p_{N_2}}{p_{NH_3}{}^2} = \frac{X_{H_2}{}^3 X_{N_2}}{X_{NH_3}{}^2}\, p^2 \tag{40}$$

$$K_{p,(25)} = \frac{p_{CO_2} p_{H_2O}{}^2}{p_{CH_4} p_{O_2}{}^2} = \frac{X_{CO_2} X_{H_2O}{}^2}{X_{CH_4} X_{O_2}{}^2} \tag{41}$$

$$K_{p,(26)} = \frac{p_{CO_2}{}^2 p_{H_2O}}{p_{C_2H_2} p_{O_2}{}^{5/2}} = \frac{X_{CO_2}{}^2 X_{H_2O}}{X_{C_2H_2} X_{O_2}{}^{5/2}} p^{-1/2} \quad (42)$$

$$K_{p,(27)} = \frac{p_{CO}{}^2 p_{H_2O}{}^2}{p_{C_2H_4} p_{O_2}{}^2} = \frac{X_{CO}{}^2 X_{H_2O}{}^2}{X_{C_2H_4} X_{O_2}{}^2} p \quad (43)$$

$$K_{p,(28)} = \frac{p_O}{p_{O_2}{}^{1/2}} = \frac{X_O}{X_{O_2}{}^{1/2}} p^{1/2} \quad (44)$$

$$K_{p,(29)} = \frac{p_H}{p_{H_2}{}^{1/2}} = \frac{X_H}{X_{H_2}{}^{1/2}} p^{1/2} \quad (45)$$

$$K_{p,(30)} = \frac{p_{OH}}{p_{H_2}{}^{1/2} p_{O_2}{}^{1/2}} = \frac{X_{OH}}{X_{H_2}{}^{1/2} X_{O_2}{}^{1/2}} \quad (46)$$

$$K_{p,(31)} = \frac{p_{H_2O}}{p_{H_2} p_{O_2}{}^{1/2}} = \frac{X_{H_2O}}{X_{H_2} X_{O_2}{}^{1/2}} p^{-1/2} \quad (47)$$

$$K_{p,(32)} = \frac{p_N}{p_{N_2}{}^{1/2}} = \frac{X_N}{X_{N_2}{}^{1/2}} p^{1/2} \quad (48)$$

$$K_{p,(33)} = \frac{p_{NO}}{p_{N_2}{}^{1/2} p_{O_2}{}^{1/2}} = \frac{X_{NO}}{X_{N_2}{}^{1/2} X_{O_2}{}^{1/2}} \quad (49)$$

$$K_{p,(34)} = p_{C(g)} = X_{C(g)}p \tag{50}$$

$$K_{p,(35)} = \frac{p_{CO}}{p_{O_2}^{1/2}} = \frac{X_{CO}}{X_{O_2}^{1/2}} p^{1/2} \tag{51}$$

$$K_{p,(36)} = \frac{p_{CO}^{2}}{p_{CO_2}} = \frac{X_{CO}^{2}}{X_{CO_2}} p \tag{52}$$

$$K_{p,(37)} = \frac{p_{H_2} p_{CO}}{p_{H_2O}} = \frac{X_{H_2} X_{CO}}{X_{H_2O}} p \tag{53}$$

$$K_{p,(38)} = \frac{p_{CN}}{p_N} = \frac{X_{CN}}{X_N} \tag{54}$$

$$K_{p,(39)} = \frac{p_{HCN} p_{H_2}}{p_{NH_3}} = \frac{X_{HCN} X_{H_2}}{X_{NH_3}} p \tag{55}$$

Equations (40) to (55) may now be used to express the mole fraction of each species in terms of the mole fractions of N_2, H_2, and CO. The resulting expressions are

$$X_{NH_3} = aX_{H_2}^{3/2} X_{N_2}^{1/2} \tag{56}$$

$$X_{CH_4} = bX_{H_2}^{2} \tag{57}$$

$$X_{C_2H_2} = cX_{H_2} \tag{58}$$

$$X_{C_2H_4} = dX_{H_2}^{2} \tag{59}$$

$$X_O = eX_{CO} \tag{60}$$

$$X_H = fX_{H_2}^{1/2} \tag{61}$$

$$X_{OH} = gX_{CO}X_{H_2}^{1/2} \tag{62}$$

$$X_{H_2O} = hX_{H_2}X_{CO} \tag{63}$$

$$X_N = iX_{N_2}^{1/2} \tag{64}$$

$$X_{NO} = jX_{N_2}^{1/2}X_{CO} \tag{65}$$

$$X_{C(g)} = k \tag{66}$$

$$X_{O_2} = lX_{CO}^{2} \tag{67}$$

$$X_{CO_2} = mX_{CO}^{2} \tag{68}$$

$$X_{CN} = nX_{N_2}^{1/2} \tag{69}$$

$$X_{HCN} = oX_{H_2}^{1/2}X_{N_2}^{1/2} \tag{70}$$

where

$$a = \frac{p}{K_{p,(24)}^{1/2}} \tag{71}$$

$$b = \frac{K_{p,(35)}^{4}p}{K_{p,(37)}^{2}K_{p,(36)}K_{p,(25)}} \tag{72}$$

$$c = \frac{K_{p,(35)}^{5}}{K_{p,(36)}^{2}K_{p,(37)}K_{p,(26)}} \tag{73}$$

$$d = \frac{K_{p,(35)}^{4}p}{K_{p,(27)}K_{p,(37)}^{2}} \tag{74}$$

$$e = \frac{K_{p,(28)}}{K_{p,(35)}} \tag{75}$$

$$f = K_{p,(29)}p^{-1/2} \tag{76}$$

$$g = \frac{K_{p,(30)}p^{1/2}}{K_{p,(35)}} \tag{77}$$

$$h = \frac{p}{K_{p,(37)}} \tag{78}$$

$$i = K_{p,(32)}p^{-1/2} \tag{79}$$

$$j = \frac{K_{p,(33)} p^{1/2}}{K_{p,(35)}} \tag{80}$$

$$k = K_{p,(34)} p^{-1} \tag{81}$$

$$l = \frac{p}{K_{p,(35)}^{2}} \tag{82}$$

$$m = \frac{p}{K_{p,(36)}} \tag{83}$$

$$n = K_{p,(38)} K_{p,(32)} p^{-1/2} \tag{84}$$

$$o = \frac{K_{p,(39)}}{K_{p,(24)}^{1/2}} \tag{85}$$

The governing equations (eqs. (13) to (16)) may now be restated as follows:

$$\tilde{K}_{N,w} = \frac{M_N}{\bar{M}} \left(a X_{H_2}^{3/2} X_{N_2}^{1/2} + j X_{N_2}^{1/2} X_{CO} + n X_{N_2}^{1/2} + i X_{N_2}^{1/2} + 2 X_{N_2} + o X_{H_2}^{1/2} X_{N_2}^{1/2} \right)_w = \frac{\tilde{K}_{N,e} h + m_N \lambda \dot{m}_c}{h + \left[1 + \lambda (1 - f) \right] \dot{m}_c} \tag{86}$$

$$\tilde{K}_{O,w} = \frac{M_O}{\bar{M}} \left(j X_{N_2}^{1/2} X_{CO} + 2l X_{CO}^{2} + 2m X_{CO}^{2} + e X_{CO} + g X_{CO} X_{H_2}^{1/2} + h X_{H_2} X_{CO} + X_{CO} \right)_w = \frac{\tilde{K}_{O,e} h + m_O \lambda \dot{m}_c}{h + \left[1 + \lambda (1 - f) \right] \dot{m}_c} \tag{87}$$

$$\tilde{K}_{C,w} = \frac{M_C}{\bar{M}}\left(bX_{H_2}^{\ 2} + X_{CO} + 2cX_{H_2} + k + mX_{CO}^{\ 2} + nX_{N_2}^{\ 1/2} + oX_{H_2}^{\ 1/2}X_{N_2}^{\ 1/2} + 2dX_{H_2}^{\ 2}\right)_w = \frac{\left[1 + \left(m_C - f\right)\lambda\right]\dot{m}_c}{h + \left[1 + \lambda(1 - f)\right]\dot{m}_c} \tag{88}$$

$$\tilde{K}_{H,w} = \frac{M_N}{\bar{M}}\left(3aX_{H_2}^{\ 3/2}X_{N_2}^{\ 1/2} + 4bX_{H_2}^{\ 2} + 2X_{H_2} + 2cX_{H_2} + fX_{H_2}^{\ 1/2} + gX_{CO}X_{H_2}^{\ 1/2} + 2hX_{H_2}X_{CO} + oX_{H_2}^{\ 1/2}X_{N_2}^{\ 1/2} + 4dX_{H_2}^{\ 2}\right)_w = \frac{m_H\lambda\dot{m}_c}{h + \left[1 + \lambda(1 - f)\right]\dot{m}_c} \tag{89}$$

Approximate Solution

General expressions.- When all the equilibrium coefficients (a, b, etc.) are <<1.0, equations (86) to (89) may be approximated as follows:

$$\tilde{K}_{N,w} = 2\frac{M_N}{\bar{M}}X_{N_2,w} = K_{N_2,w} = \frac{\tilde{K}_{N,e}h + m_N\lambda\dot{m}_c}{h + \left[1 + \lambda(1 - f)\right]\dot{m}_c} \tag{90}$$

$$\tilde{K}_{O,w} = \frac{M_O}{\bar{M}}X_{CO,w} = \frac{M_O}{M_{CO}}K_{CO,w} = \frac{\tilde{K}_{O,e}h + m_O\lambda\dot{m}_c}{h + \left[1 + \lambda(1 - f)\right]\dot{m}_c} \tag{91}$$

$$\tilde{K}_{C,w} = \frac{M_C}{\bar{M}}X_{CO,w} = \frac{M_C}{M_{CO}}K_{CO,w} = \frac{\left[1 + \left(m_C - f\right)\lambda\right]\dot{m}_c}{h + \left[1 + \lambda(1 - f)\right]\dot{m}_c} \tag{92}$$

$$\tilde{K}_{H,w} = \frac{2M_H}{\bar{M}}X_{H_2,w} = K_{H_2,w} = \frac{m_H\lambda\dot{m}_c}{h + \left[1 + \lambda(1 - f)\right]\dot{m}_c} \tag{93}$$

and equations (91) and (92) may be solved for $\dot{m}_c$ as follows:

$$\dot{m}_c = \frac{h\tilde{K}_{O,e}}{W} \tag{94}$$

where

$$W = \frac{M_O}{M_C}\left[1 + (m_C - f)\lambda\right] - m_O\lambda \tag{95}$$

It should be noted that the solution for $\dot{m}_c$, presented in equations (94) and (95), is valid for the general case of transient ablation. The parameter W is, however, a function of λ and in the transient case λ is not known but must be obtained from experiment or through the iterative solution of a transient ablation computer program. For the steady-state ablation case, however, λ is a known constant. The steady-state ablation case is considered in detail in the subsequent section of this paper.

The boundary-layer composition at the char surface can be obtained from equations (90), (91), and (93) as follows:

$$K_{N_2,w} = \frac{W\dfrac{\tilde{K}_{N,e}}{\tilde{K}_{O,e}} + m_N\lambda}{\dfrac{W}{\tilde{K}_{O,e}} + 1 + \lambda(1 - f)} \tag{96}$$

$$K_{CO,w} = \frac{\dfrac{M_{CO}}{M_O}\left[W + m_O\lambda\right]}{\dfrac{W}{\tilde{K}_{O,e}} + 1 + \lambda(1 - f)} \tag{97}$$

$$K_{H_2,w} = \frac{m_H\lambda}{\dfrac{W}{\tilde{K}_{O,e}} + 1 + \lambda(1 - f)} \tag{98}$$

The mass fractions $K_{i,w}$ can, of course, be expressed in terms of mole fractions $X_{i,w}$ through the relation

$$X_i = \frac{\frac{K_i}{M_i}}{\sum_j \frac{K_j}{M_j}} \tag{99}$$

Once the boundary-layer composition at the char surface has been determined, an overall heat of reaction may be calculated as follows. An equation for the overall reaction per mole of boundary-layer gas mixture may be written as

$$\left[AO_2 + BN_2\right] + \left[C\left(CO + \frac{\bar{X}_{CO_2}}{\bar{X}_{CO}} CO_2 + \frac{\bar{X}_{CH_4}}{\bar{X}_{CO}} CH_4 + \frac{\bar{X}_{C_2H_2}}{\bar{X}_{CO}} C_2H_2 + \frac{\bar{X}_{C_2H_4}}{\bar{X}_{CO}} C_2H_4 \right.\right.$$

$$\left.\left. + \frac{\bar{X}_{N_2}}{\bar{X}_{CO}} N_2 + \frac{\bar{X}_{NH_3}}{\bar{X}_{CO}} NH_3 + \frac{\bar{X}_{H_2O}}{\bar{X}_{CO}} H_2O + \frac{\bar{X}_{H_2}}{\bar{X}_{CO}} H_2\right)\right]$$

$$+ \left[DC(s)\right] \rightleftharpoons \left[X_{N_2,w}N_2 + X_{CO,w}CO + X_{H_2,w}H_2\right] \tag{100}$$

where $\bar{X}_i$ is the number of moles of species i per mole of pyrolysis gas. The terms of equation (100) are identified as follows:

$$\left[\text{Species from stream}\right] + \left[\text{Pyrolysis gases}\right] + \left[\text{Char}\right] \rightleftharpoons \left[\text{Reaction products}\right]$$

The requirement that the number of atoms of a given element must be the same on both sides of equation (100) results in the following relations:

$$2A + C\left(1 + \frac{2\bar{X}_{CO_2}}{\bar{X}_{CO}} + \frac{\bar{X}_{H_2O}}{\bar{X}_{CO}}\right) = X_{CO,w} \tag{101}$$

$$2B + C\left(\frac{2\bar{X}_{N_2}}{\bar{X}_{CO}} + \frac{\bar{X}_{NH_3}}{\bar{X}_{CO}}\right) = 2X_{N_2,w} \tag{102}$$

$$C\left(1+\frac{\bar{X}_{CO_2}}{\bar{X}_{CO}}+\frac{\bar{X}_{CH_4}}{\bar{X}_{CO}}+\frac{2\bar{X}_{C_2H_2}}{\bar{X}_{CO}}+\frac{2\bar{X}_{C_2H_4}}{\bar{X}_{CO}}\right)+D=X_{CO,w} \tag{103}$$

$$C\left(\frac{4\bar{X}_{CH_4}}{\bar{X}_{CO}}+\frac{2\bar{X}_{C_2H_2}}{\bar{X}_{CO}}+\frac{4\bar{X}_{C_2H_4}}{\bar{X}_{CO}}+\frac{3\bar{X}_{NH_3}}{\bar{X}_{CO}}+\frac{2\bar{X}_{H_2O}}{\bar{X}_{CO}}+\frac{2\bar{X}_{H_2}}{\bar{X}_{CO}}\right)=2X_{H_2,w} \tag{104}$$

but, for each mole of reaction products produced, $N_A C\left(1+\frac{2\bar{X}_{CO_2}}{\bar{X}_{CO}}+\frac{\bar{X}_{H_2O}}{\bar{X}_{CO}}\right)$ oxygen atoms entered the reaction in the form of pyrolysis gases and $N_A D$ atoms of carbon entered the reaction in the form of char. Hence, from the definition of f and m_O,

$$\frac{C\left(1+\frac{2\bar{X}_{CO_2}}{\bar{X}_{CO}}+\frac{\bar{X}_{H_2O}}{\bar{X}_{CO}}\right)}{D}=\frac{m_O M_C \lambda}{M_O} \tag{105}$$

Similarly,

$$\frac{C\left(1+\frac{\bar{X}_{CO_2}}{\bar{X}_{CO}}+\ldots\right)}{D}=\left(m_C-f\right)\lambda \tag{106}$$

$$\frac{C\left(\frac{4\bar{X}_{CH_4}}{\bar{X}_{CO}}+\ldots\right)}{D}=\frac{m_H M_C \lambda}{M_H} \tag{107}$$

$$\frac{C\left(\frac{2\bar{X}_{N_2}}{\bar{X}_{CO}}+\ldots\right)}{D}=\frac{m_N M_C \lambda}{M_N} \tag{108}$$

and equations (101), (102), (103), and (104) with the aid of equations (105) to (108) can be expressed per mole of C(s) (char) by dividing through by D. Hence,

$$\frac{2A}{D} + \frac{m_O M_C \lambda}{M_O} = \frac{X_{CO,w}}{D} \tag{109}$$

$$\frac{2B}{D} + \frac{m_N M_C \lambda}{M_N} = \frac{2X_{N_2,w}}{D} \tag{110}$$

$$\left(m_C - f\right)\lambda + 1 = \frac{X_{CO,w}}{D} \tag{111}$$

$$\frac{m_H M_C \lambda}{M_H} = \frac{2X_{H_2,w}}{D} \tag{112}$$

Since the overall heat of reaction is defined as

$$\Delta H_R = \text{Enthalpy of products - Enthalpy of reactants}$$

from equation (100), the overall heat of reaction per mole of solid carbon (char) consumed may be stated as

$$\Delta H_R = \frac{X_{CO,w}}{D}\Delta H_{f,CO} - \frac{C}{D\bar{X}_{CO}}\left(\bar{X}_{CO}\Delta H_{f,CO} + \bar{X}_{CO_2}\Delta H_{f,CO_2} + \bar{X}_{CH_4}\Delta H_{f,CH_4}\right.$$

$$\left. + \bar{X}_{C_2H_2}\Delta H_{f,C_2H_2} + \bar{X}_{C_2H_4}\Delta H_{f,C_2H_4} + \bar{X}_{NH_3}\Delta H_{f,NH_3} + \bar{X}_{H_2O}\Delta H_{f,H_2O}\right) \tag{113}$$

but according to equations (111) and (105)

$$\frac{X_{CO,w}}{D} = \left(m_C - f\right)\lambda + 1 \tag{114}$$

$$\frac{C}{D\bar{X}_{CO}} = \frac{m_O M_C \lambda}{M_O} \frac{1}{\bar{X}_{CO} + 2\bar{X}_{CO_2} + \bar{X}_{H_2O}} \tag{115}$$

Hence equation (113) becomes

$$\Delta H_R = \left[\left(m_C - f\right)\lambda + 1\right] \Delta H_{f,CO} - \frac{m_O M_C \lambda}{M_O} \frac{\sum_i \bar{X}_i \Delta H_{f,i}}{\bar{X}_{CO} + 2\bar{X}_{CO_2} + \bar{X}_{H_2O}} \tag{116}$$

The heat flux due to chemical reactions (recombination reactions for oxygen and nitrogen are not included since they are usually accounted for in computing convective heat fluxes) may now be expressed as

$$q_{ch} = -\frac{\Delta H_R \dot{m}_c}{M_C} = -\frac{h\tilde{K}_{O,e}}{M_C W}\left\{\left[\left(m_C - f\right)\lambda + 1\right] \Delta H_{f,CO} - \frac{m_O M_C \lambda}{M_O} \frac{\sum_i \bar{X}_i \Delta H_{f,i}}{\bar{X}_{CO} + 2\bar{X}_{CO_2} + \bar{X}_{H_2O}}\right\} \tag{117}$$

(The minus sign is used in equation (117) since, by definition, an exothermic reaction has a negative heat of reaction.) Equation (117) may now be used to define an "effective chemical enthalpy potential ΔH_{ch}" as follows:

$$\Delta H_{ch} = \frac{q_{ch}}{h} = -\frac{\tilde{K}_{O,e}}{M_C W}\left\{\left[\left(m_C - f\right)\lambda + 1\right] \Delta H_{f,CO} - \frac{m_O M_C \lambda}{M_O} \frac{\sum_i \bar{X}_i \Delta H_{f,i}}{\bar{X}_{CO} + 2\bar{X}_{CO_2} + \bar{X}_{H_2O}}\right\} \tag{118}$$

Hence, the total heat flux (convective + chemical) is expressible as

$$q_t = h\left(\Delta H + \Delta H_{ch}\right) \tag{119}$$

Since expressions for the gas composition at the char surface have been derived, consideration of the transpiration cooling effect produced by the pyrolysis gases is of interest. In practical applications the reduction in heat transfer which results from the injection of gas into the boundary layer is often accounted for by using the relation

$$h = h^{o} - \eta(\rho v)_{w} \tag{120}$$

and in reference 10 it is suggested that the transpiration factor η varies approximately as $\hat{M}^{-l}$ where $\hat{M}$ is the molecular weight of the injected gas and l ranges from 1/3 to 1/4. If the gas phase combustion reactions all occur near the char surface, the species which are actually injected into the boundary layer are the combustion products, that is, N_2, H_2, and CO. The mass fraction of N_2 in the injected gases is expressible as

$$\hat{K}_{N_2} = \frac{\dot{m}_{N_2}}{(\rho v)_{w}} = \frac{m_N \dot{m}_{vp}}{(1 - f)\dot{m}_{vp} + \dot{m}_{c}} = \frac{m_N \lambda}{(1 - f)\lambda + 1} \tag{121}$$

and similarly

$$\hat{K}_{H_2} = \frac{\dot{m}_{H_2}}{(\rho v)_{w}} = \frac{m_H \dot{m}_{vp}}{(1 - f)\dot{m}_{vp} + \dot{m}_{c}} = \frac{m_H \lambda}{(1 - f)\lambda + 1} \tag{122}$$

$$\hat{K}_{CO} = \frac{\dot{m}_{CO}}{(\rho v)_{w}} = \frac{(m_O + m_C - f)\dot{m}_{vp} + \dot{m}_{c}}{(1 - f)\dot{m}_{vp} + \dot{m}_{c}} = \frac{(m_O + m_C - f)\lambda + 1}{(1 - f)\lambda + 1} \tag{123}$$

Hence, the average molecular weight of the injected gases is given by the expression

$$\hat{M} = \frac{(1 - f)\lambda + 1}{\frac{m_N \lambda}{M_{N_2}} + \frac{m_H \lambda}{M_{H_2}} + \frac{(m_O + m_C - f)\lambda + 1}{M_{CO}}} \tag{124}$$

Now the ratio of the transpiration cooling factor for a gas of arbitrary molecular weight to the transpiration cooling factor for carbon monoxide (M = 28) is

$$\frac{\eta}{\eta_{\hat{M}=28}} = \left(\frac{\hat{M}}{28}\right)^{-l} = \left[\frac{(1 - f)\lambda + 1}{m_N\lambda + 14m_H\lambda + m_O\lambda + m_C\lambda - f\lambda + 1}\right]^{-l} = \left[1 + \frac{13m_H\lambda}{(1 - f)\lambda + 1}\right]^{l} \tag{125}$$

and since for a laminar boundary layer

$$\eta_{\hat{M}=28} \approx \eta_{air} \approx 0.7 \tag{126}$$

equation (120) may be approximated by the following expression

$$h \approx h^{O} - 0.7\left[1 + \frac{13m_H\lambda}{(1 - f)\lambda + 1}\right]^{l} (\rho v)_w \tag{127}$$

Steady-state expressions.- The solutions obtained in this analysis (as presented in eqs. (94) to (98), (116) to (119), and (127)) are applicable to the case of transient ablation - that is, the case where the char surface and the pyrolysis interface move at different linear rates. However, these solutions depend on the ratio of pyrolysis rate to char oxidation rate λ, and λ is not known a priori except in the case of steady-state ablation where $\lambda = 1/f$. The limiting case of steady ablation is, however, an important one and hence the solutions for $\lambda = 1/f$ are presented in the following equations:

$$\frac{\dot{m}_c}{f} = \dot{m}_{vp} = \frac{\tilde{K}_{O,e}h}{fW^*} \tag{128}$$

where

$$fW^* = \frac{M_O}{M_C}m_C - m_O = \frac{M_O(\sigma - \varphi)}{\sigma M_C + \tau M_H + \nu M_N + \varphi M_O} \tag{129}$$

$$K_{N_2,w} = 1 - \left(1 + \frac{M_C}{M_{CO}}\frac{m_H}{m_C}\right)K_{CO,w} = 1 - \left(1 + \frac{\tau}{28\sigma}\right)K_{CO,w} \tag{130}$$

$$K_{H_2,w} = \frac{M_C}{M_{CO}} \frac{m_H}{m_C} K_{CO,w} = \frac{\tau}{28\sigma} K_{CO,w} \tag{131}$$

$$K_{CO,w} = \frac{\frac{28}{16}\left(fW^* + m_O\right)}{\frac{fW^*}{\tilde{K}_{O,e}} + 1} \tag{132}$$

$$\Delta H_R = \frac{m_C}{f} \Delta H_{f,CO} - \frac{m_O}{f} \frac{3}{4}\left(\frac{\sum_i \bar{X}_i \Delta H_{f,i}}{\bar{X}_{CO} + 2\bar{X}_{CO_2} + \bar{X}_{H_2O}}\right) \tag{133}$$

$$\Delta H_{ch} = \frac{q_{ch}}{h} = -\frac{\tilde{K}_{O,e}}{12\left(\frac{4}{3} m_C - m_O\right)}\left(m_C \Delta H_{f,CO} - \frac{\frac{3}{4} m_O \sum_i \bar{X}_i \Delta H_{f,i}}{\bar{X}_{CO} + 2\bar{X}_{CO_2} + \bar{X}_{H_2O}}\right)$$

$$= -\frac{\tilde{K}_{O,e}}{16(\sigma - \varphi)}\left(\sigma \Delta H_{f,CO} - \frac{\varphi \sum_i \bar{X}_i \Delta H_{f,i}}{\bar{X}_{CO} + 2\bar{X}_{CO_2} + \bar{X}_{H_2O}}\right) \tag{134}$$

$$h = h^o - \eta \dot{m}_{vp} = h^o - 0.7\left(1 + 13 m_H\right)^l \dot{m}_{vp} \tag{135}$$

DISCUSSION

In this section, the assumptions used in the analysis are reviewed, a physical interpretation of the approximate solution is presented, and the effects of virgin plastic composition and pyrolysis gas composition on the char oxidation rate, the steady-state ablation rate, the cold-wall effective heat of ablation (defined subsequently), and the heat release due to chemical reactions are discussed. In the section "Analysis," both general and steady-state expressions of the approximate solution were presented. Before a

solution to the general expressions can be obtained, the ratio of pyrolysis rate to char oxidation rate λ (which is not known except for the steady-state ablation case) must be specified. Hence, while the general expressions can be used in conjunction with a computer program (such as that presented in ref. 11) to yield transient ablation rates, they do not lend themselves to demonstrating the general characteristics of diffusion-controlled char oxidation. For steady-state ablation, on the other hand, $\lambda = 1/f$ and as a result the equations are simple and provide a clear physical picture of diffusion-controlled char oxidation. Accordingly, the following discussion is restricted to the steady-state case. Any remarks concerning the char oxidation rate apply equally well to the virgin-plastic ablation rate since $\dot{m}_c = f\dot{m}_{vp}$.

Review of Assumptions

The major assumptions used in the present analysis are:

(a) The virgin material is composed of only oxygen, hydrogen, nitrogen, and carbon.

(b) The mass-transfer coefficients for all gas phase species are numerically equal to the convective heat-transfer coefficient.

(c) All the equilibrium constants in equations (86) to (89) are $<<1.0$.

(d) Chemical equilibrium (both gas phase and heterogeneous) is obtained at the char surface.

(e) The transpiration factor η varies inversely with the kth power of the mean molecular weight of the gases injected into the boundary layer.

(f) The pyrolysis gases are composed of N_2, H_2, NH_3, CO, CO_2, C_2H_4, C_2H_2, CH_4, and H_2O.

Most presently used high-temperature resins (silicone resins and rubber are notable exceptions) are composed of O, H, and C. Nylon, which is commonly used as a reinforcement in ablative materials, is composed of O, H, N, and C; hence, mixtures such as epoxy nylon or phenolic nylon can be treated by the techniques presented herein. Also, the present method could be applied to a material composed of a hydrocarbon resin and an inert filler.

The assumption made in evaluating the mass-transfer coefficients is commonly made in analyses of carbon combustion. (See refs. 2, 3, 7, 8, and 9.) In reference 9 this assumption is shown to be valid whenever the gas mixture can be considered binary with respect to diffusion and the Lewis number is unity. Even though neither of these requirements are rigorously met for carbon combustion, use of the mass-transfer-coefficient assumption yields results which are in qualitative agreement with experiment.

A measure of the validity of this assumption for carbon combustion can be obtained by comparing the present solution with that presented in references 1 and 4. The analysis presented in references 1 and 4 considered multicomponent diffusion and placed no restriction on Lewis number. From that analysis the following expression for the diffusion-controlled stagnation-point carbon oxidation rate in air was obtained and presented in reference 4:

$$\dot{m}_c\sqrt{\frac{r}{p_e}} = 6.35 \times 10^{-3} \text{ lb/ft}^{3/2}\text{-sec-atm}^{1/2} = 0.05378 \times 10^{-3} \text{ kg/m}^{1/2}\text{-N}^{1/2}\text{-sec} \qquad (136)$$

Before the results of the present analysis can be compared with equation (136) a value for the heat-transfer coefficient must be obtained. Evaluation of the Fay and Riddell relation (ref. 12) has shown that values on the order of

$$h^o\sqrt{\frac{r}{p_e}} = 3.92 \times 10^{-2} \text{ lb/ft}^{3/2}\text{-sec-atm}^{1/2} = 0.033198 \times 10^{-2} \text{ kg/m}^{1/2}\text{-N}^{1/2}\text{-sec} \qquad (137)$$

are typical of stagnation-point conditions on a manned vehicle during entry from earth orbit. If this value and the oxygen mass fraction for air (0.232) are substituted into equations (94), (95), and (127) there results,

$$\dot{m}_c\sqrt{\frac{r}{p_e}} = 6.07 \times 10^{-3} \text{ lb/ft}^{3/2}\text{-sec-atm}^{1/2} = 0.051407 \times 10^{-3} \text{ kg/m}^{1/2}\text{-N}^{1/2}\text{-sec} \qquad (138)$$

which agrees with equation (136) to within 5 percent. The total heat flux calculated from equation (119) was also found to agree with the values presented in references 1 and 4 to within 5 percent. Hence the unity Lewis number assumption may be considered valid for carbon combustion. Only the presence of light gases (primarily H_2) makes the assumption less applicable to the present analysis than to carbon combustion. Hence the assumption should be quite good for low values of free-stream oxygen mass fraction $\left(\text{as } \tilde{K}_{O,e} \to 0 \text{ and } \tilde{K}_{H_2,w} \to 0, \text{ eq. (98)}\right)$ and although the validity of the assumption decreases with increasing $\tilde{K}_{O,e}$, it should provide an acceptable qualitative description of the transport process for air. This assumption is considered in the light of calculated char-surface boundary-layer compositions subsequently.

The approximate solution was obtained by assuming that the equilibrium coefficients appearing in equations (86) to (89) were small compared with unity. A more rigorous statement of this requirement would be that the sum of all the equilibrium coefficients appearing in a given equation must be small compared with unity. In order to assess the validity of this assumption, the equilibrium coefficients were evaluated by using the data presented in reference 16. The variation of these coefficients (evaluated for a pressure of 1 atm) with temperature is presented in figure 2. By using the curves presented in figure 2, ranges of char surface temperature and pressure for which the sum of the equilibrium coefficients appearing in any one of equations (86) to (89) was $\lesssim 0.1$ were identified.

The ranges of char surface temperature and pressure within which the sum of these coefficients is $\lesssim 0.1$ (and, hence, within which the approximate solution is valid) are presented in figure 3. The char surface temperatures and pressures experienced by a manned ballistic vehicle (such as the Mercury spacecraft) during entry from earth orbit fall within this range and hence the present approximate solution should be applicable to such vehicles. On the other hand, ballistic missiles and lunar return vehicles experience temperatures higher than those shown in the cross-hatched region of figure 3. Solution of the governing equations at these higher temperatures is straightforward but would require the use of a digital computer.

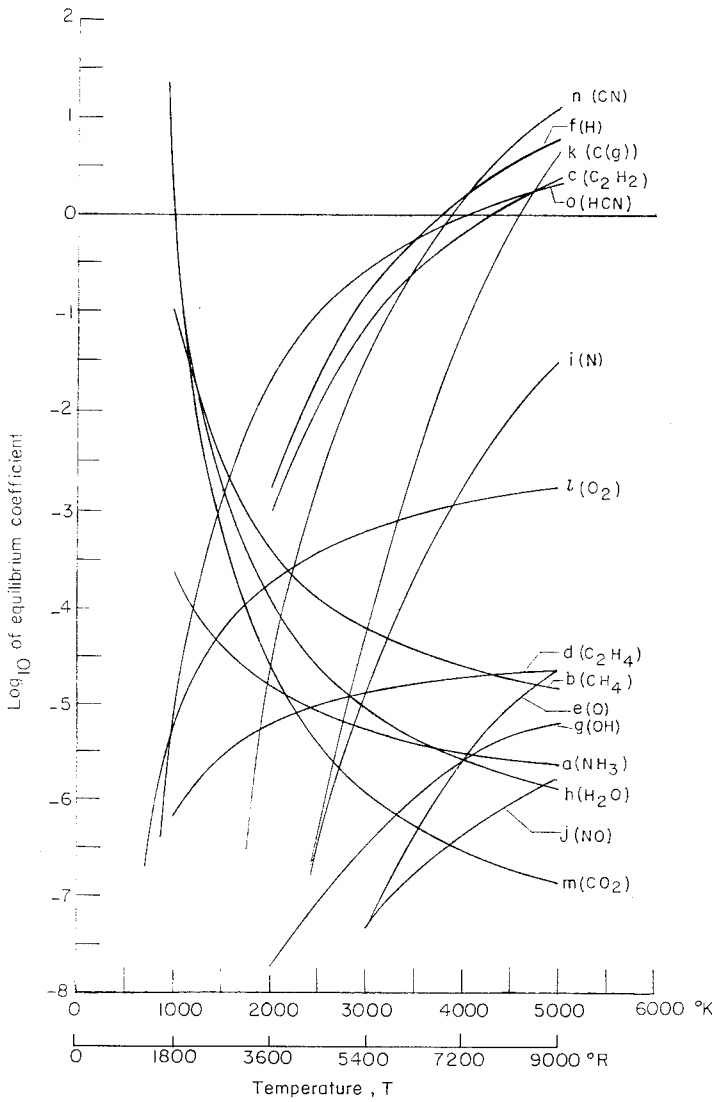

Figure 2.- Variation with temperature of equilibrium coefficients. Pressure, 1 atm (0.1013 MN/m^2).

The assumption of chemical equilibrium at the char surface is a natural consequence of considering the case of diffusion-controlled char oxidation. In any kinetic system, the slowest step is rate controlling. Hence, in the diffusion-controlled case, the rate of transport of reactants must be slow compared to the rates of both homogeneous and heterogeneous reactions. Since the time required for the slowest reaction to equilibrate is small compared with the time required to deliver fresh quantities of reactants to the char surface, chemical equilibrium is obtained.

The assumption made with regard to the transpiration factor η is semiempirical in nature and is based on experiments and analyses involving nonreacting boundary layers. This assumption would be applicable to the present problem if all the gas phase

reactions occurred in a thin zone near the char surface. When this situation occurs, the gases injected into the boundary layer are the reaction products which diffuse from the reaction zone through the boundary layer without undergoing further reaction. It should be noted that, in analyzing reentry heating, several investigators have assumed a frozen boundary layer and local chemical equilibrium at the vehicle surface. (See, for instance, ref. 1.) This assumption is equivalent to assuming a thin reaction zone near the char surface. When reactions occur throughout the boundary layer, the present approach is not applicable; however, to the author's knowledge, no solutions for the transpiration effect of pyrolysis gases injected into a reacting boundary layer are available. Certainly, there exists the possibility that transpiration cooling effects significantly different from those predicted by equations (120) to (127) will be obtained. As the following discussion develops, however, it will be seen that transpiration factors which differed from the presently used values by factors of two or even three would not significantly change the qualitative results of this analysis. Hence the present assumption is reasonably accurate for the case of frozen boundary layers with chemical equilibrium at the char surface and could in no case introduce errors which would significantly alter the conceptual picture of diffusion-controlled char oxidation presented herein.

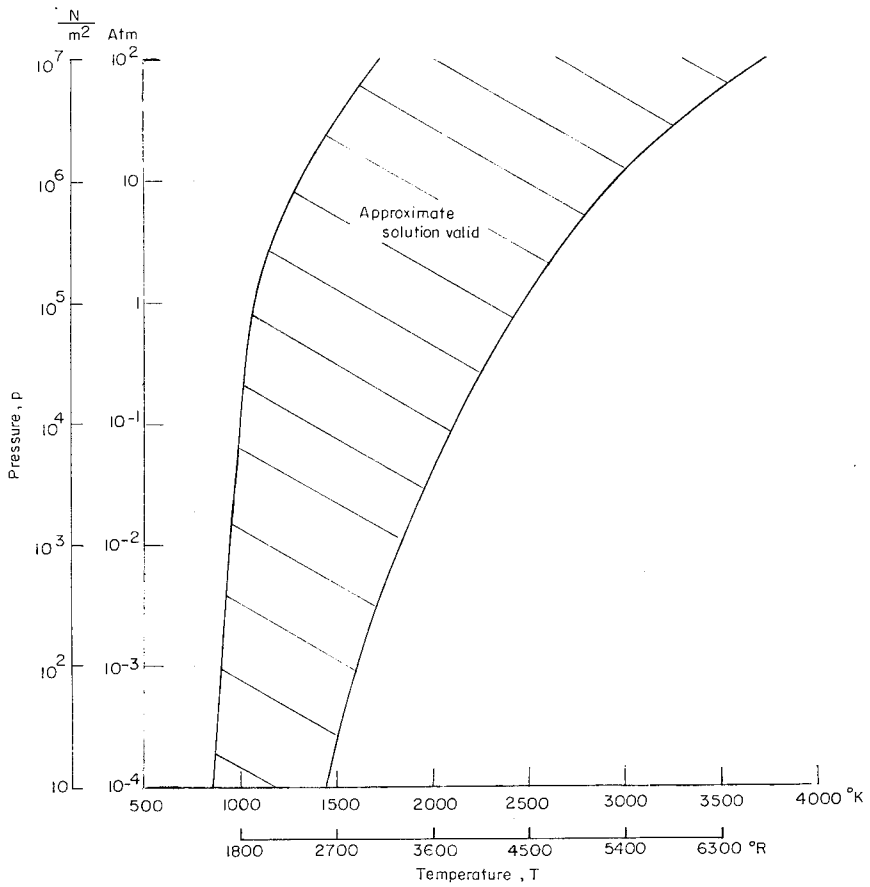

Figure 3.- Range of validity for approximate solution.

The pyrolysis gases assumed in the present treatment represent the major species which have most often been reported by chemists who have attempted experimentally to determine pyrolysis gas compositions. (See, for instance, refs. 13 and 14.) The pyrolysis gases considered in the present report are those which reach the char surface. Hence, while the initial decomposition of the plastic may produce large molecular weight

hydrocarbon species, it is assumed that cracking reactions in the char reduce these large fragments to the species listed in assumption (f).

Pyrolysis gas compositions, calculated for the equilibrium decomposition (i.e., all cracking reactions in chemical equilibrium) of phenolic nylon are presented in reference 15 and contain several species not included in assumption (f). The inclusion of all the species presented in reference 15 in the present analysis might possibly result in small changes in the region of validity shown in figure 3. The species included in assumption (f) do, however, account for approximately 90 percent (on a mass basis) of the gas mixture presented in reference 15 at temperatures near the middle of the range of validity presented in figure 3. At the low and high temperature extremes of the range of validity, the respective percentages of this gas mixture accounted for are approximately 80 and 70. Hence, the presently assumed pyrolysis gases are considered to be a reasonable approximation for the case where the cracking reactions approach equilibrium. If, on the other hand, the cracking reactions were kinetically slow so that large molecular weight hydrocarbon species reached the char surface, the pyrolysis gases in assumption (f) would be incorrect and the presence of heavy gases would cause the boundary-layer gas mixture to deviate still further from an effectively binary mixture. The fact that the major pyrolysis gas species measured experimentally (refs. 13 and 14) and calculated (ref. 15) are the same strongly suggests that char layer cracking reactions approach equilibrium.

Physical Interpretation of Approximate Solution

A physical interpretation of the approximate solution may be obtained from an examination of equations (128) and (129). The numerator of equation (128) is the well-known expression for the diffusion-controlled oxygen flux and is the maximum rate at which oxygen can be transported across the boundary layer to the reacting char surface. Since equation (128) is an expression for the steady-state ablation rate, fW^* must represent the mass of oxygen used in ablating a unit mass of virgin plastic. If every carbon atom initially present in the virgin plastic is assumed to react with the oxygen in the virgin plastic to form CO, then the term $\frac{\sigma - \varphi}{\sigma M_C + \tau M_H + \nu M_N + \varphi M_O}$ represents the number of moles of carbon per unit mass of virgin plastic available to react with oxygen diffusing through the boundary layer. Hence fW^* (eq. (129)) represents the mass of oxygen from external sources required to react all the carbon in a unit mass of virgin plastic to produce CO. This, then, is the physical interpretation of the approximate solution: all the carbon present in the virgin plastic is reacted to form CO and the reaction rate is determined by the rate at which oxygen can be supplied by pyrolysis of the virgin plastic plus diffusion through the boundary layer. It is in this respect that the present analysis differs

most significantly from previous analyses of char oxidation and carbon combustion. In these previous analyses, only the carbon present in the char layer is considered reactable.

Effect of Virgin Plastic Composition on Boundary-Layer Composition at the Char Surface, Char Oxidation Rate, Ablation Rate, and Effective Heat of Ablation

The effect of virgin plastic composition on pyrolysis rate is shown by equations (128) and (129). However, the transfer coefficient h which appears in equation (128) is dependent on the virgin plastic hydrogen content as shown in equation (135). When equation (135) is substituted into equation (128), the following relation is obtained:

$$\dot{m}_{vp} = \frac{\dot{m}_c}{f} = \frac{\tilde{K}_{O,e} h^o}{fW^* + \tilde{K}_{O,e}\eta} = \frac{\tilde{K}_{O,e} h^o}{fW^* + 0.7\left(1 + 13m_H\right)^{\frac{1}{2}} \tilde{K}_{O,e}} \tag{139}$$

Equation (139) indicates that $\dot{m}_{vp}$ decreases with increasing fW^* and increasing transpiration factor η. Since fW^* increases with increasing virgin plastic carbon content and decreasing oxygen, nitrogen, and hydrogen content and η increases with increasing virgin plastic hydrogen content, the question arises as to whether the lowest pyrolysis rate would be obtained from a material with a high carbon content or a high hydrogen content. In an attempt to answer this question, equation (139) was used to make calculations of $\dot{m}_{vp}$ for a material which contained only carbon and hydrogen. (Eq. (129) shows that the presence of oxygen or nitrogen in the virgin plastic always produces higher pyrolysis rates.) The results of these calculations are presented in figure 4 as plots of $\dot{m}_{vp}/h^o$ against m_C for $\tilde{K}_{O,e} = 0.050$ and 0.232 and $l = 1/3$. For a specified flow environment $\left(h^o \text{ and } \tilde{K}_{O,e}\right)$, the minimum value of $\dot{m}_{vp}$ is obtained from a material which is

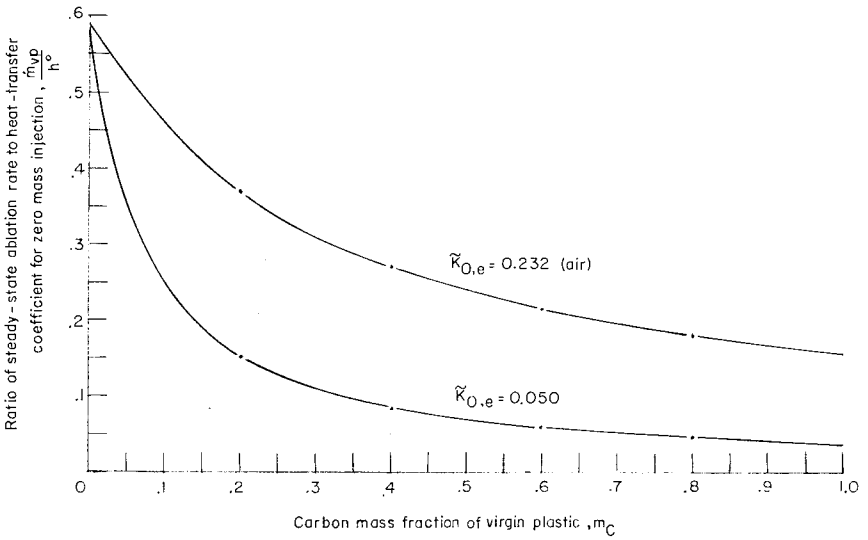

Figure 4.- Variation of dimensionless steady-state ablation rate with carbon mass fraction for plastic which contains only carbon and hydrogen.

composed entirely of carbon. Numerous investigators have impregnated porous carbon materials with hydrocarbon resins in the hope that the transpiration cooling effect produced by the vaporization of the resin would reduce the mass loss rate of the material. The results of this study show that, within the framework of the assumption presented earlier, the effect of impregnating a porous carbon with hydrocarbon resins would be to increase rather than reduce the mass loss rate.

In order to illustrate the effects of virgin plastic composition, calculations of char oxidation rate, ablation rate, and char surface boundary-layer composition were carried out for four typical hydrocarbon resins and graphite. The empirical formulas and associated parameters used in these calculations are presented in table I. The indices in the empirical formulas have been adjusted to give the numbers of carbon and hydrogen atoms per atom of oxygen and the materials are listed in order of decreasing carbon content. As pointed out previously the parameter fW^* represents the mass of oxygen required to ablate a unit mass of virgin plastic. (For graphite, no pyrolysis is involved and hence fW^* represents the mass of oxygen required to oxidize a unit mass of graphite.) The values presented in table I show that fW^* increases markedly as the relative carbon content of the material increases. The symbol m_H represents the mass of hydrogen per unit mass of virgin plastic and is related to the transpiration cooling factor η by equation (125). The significant point to be made with the values presented in table I is that while m_H differs significantly for the five materials considered,

TABLE I

EMPIRICAL FORMULAS AND ASSOCIATED PARAMETERS FOR GRAPHITE AND FOUR TYPICAL HYDROCARBON PLASTICS

Material	Empirical formula	fW^*	m_H	η (a)
Graphite	C	1.333	0	0.700
Epoxy resin	$C_{6.5} H_{7.34} O_1$	.869	.0725	.874
Phenolic resin	$C_{5.16} H_5 O_1$	.802	.0602	.849
Polyester resin	$C_{2.5} H_2 O_1$	.500	.0416	.810
Cellulose	$C_{1.2} H_2 O_1$	.099	.0617	.851

[a]In the calculation of η (see eq. (125)), the exponent l was assumed to be 1/3.

the maximum variation in η is only 25 percent. This again indicates that large increases in the transpiration cooling effect will not be obtained by increasing the hydrogen content of a plastic.

By using the empirical formulas presented in table I and equations (130), (131), and (132), the boundary-layer compositions at the char surface during the steady ablation of cellulose, polyester, phenolic, and epoxy resins, and a completely carbonaceous material were calculated and are presented in figure 5 as variations of N_2, H_2, or CO mass fraction with free-stream oxygen mass fraction. The char surface boundary-layer compositions are comparable for all the materials except cellulose. Cellulose, with its high oxygen and hydrogen contents, produces much larger quantities of CO and H_2 than the other materials do. The curves presented in figure 5 show that (with the exception of cellulose) the boundary-layer composition for the plastics is similar to that produced by graphite $\left(\text{i.e., } K_{H_2} << K_{CO} \text{ and } K_{N_2}\right)$. One of the principal assumptions involved in the present analysis is that the unity Lewis number heat-mass transfer analogy is valid. It is generally agreed that the unity Lewis number assumption is reasonably valid for carbon oxidation. (See ref. 9.) The comparable boundary-layer composition shown in figure 5 for epoxy and phenolic resins and graphite suggests that the unity Lewis number assumption may be a reasonable approximation for the present case.

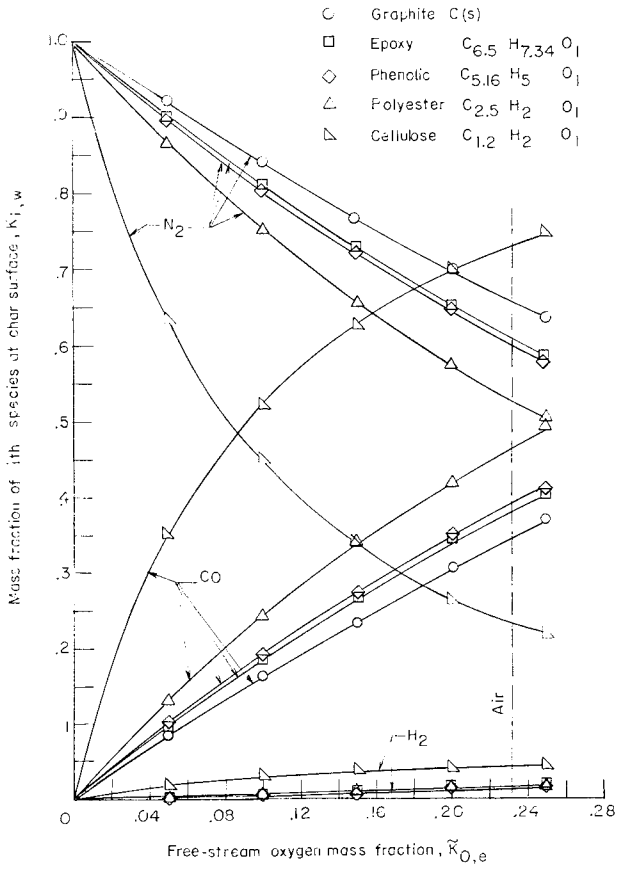

Figure 5.- Effect of virgin plastic composition on the variation of boundary-layer composition at the char surface with free-stream oxygen mass fraction.

The effect of virgin plastic composition on steady-state ablation rate is illustrated in figure 6, where ratios of ablation rate to $\tilde{K}_{O,e}h^O$ are plotted against oxygen mass fraction, $\tilde{K}_{O,e}$. The data are presented in this manner since the product $\tilde{K}_{O,e}h^O$ represents the maximum rate at which oxygen can be transported by diffusion to the char surface and hence characterizes the flow environment. The ratio $\dot{m}_{vp}/\tilde{K}_{O,e}h^O$ indicates the ablator's vulnerability to oxidation. The curve for graphite is included since it

represents (as demonstrated earlier) the minimum ablation rate attainable by a hydrocarbon material. The curves presented in figure 6 show that plastics exhibit a range of carbon content which causes significant differences in char oxidation rates and ablation rates. The ablation rates calculated for phenolic and epoxy resins (the two plastics most commonly used in ablative heat shields) are about 1.4 to 1.6 times as large as the theoretical minimum rates (for graphite), and the values for polyester and cellulose exceed those for graphite by factors of from 2.7 to 3 and 5 to 12, respectively. From time to time it has been suggested, in the literature, that wood (which is primarily cellulose) might be an acceptable ablator. The calculations presented in figure 6, however, indicate that cellulose would not be an acceptable material for flight regimes where steady ablation and diffusion-controlled char oxidation are obtained. Of the three resins, phenolic, epoxy, and polyester, the present results indicate that phenolic and epoxy would be the least vulnerable to oxidation and indeed these are the two resins most commonly used in ablative heat shields. Even though phenolics and epoxys are relatively efficient ablators, the curves presented in figure 6 predict that completely carbonaceous materials (such as prepyrolyzed resins) would have mass-loss rates that were from 60 to 70 percent of the rates obtainable from phenolics and epoxys. Most carbonaceous materials have relatively high thermal conductivities and densities and hence are poor insulators. The proper interpretation of the curves presented in figure 6 is, then, that if completely carbonaceous materials with insulating capabilities comparable to those of plastics could be developed, then these carbonaceous materials would be superior ablators by virtue of these lower mass loss rates.

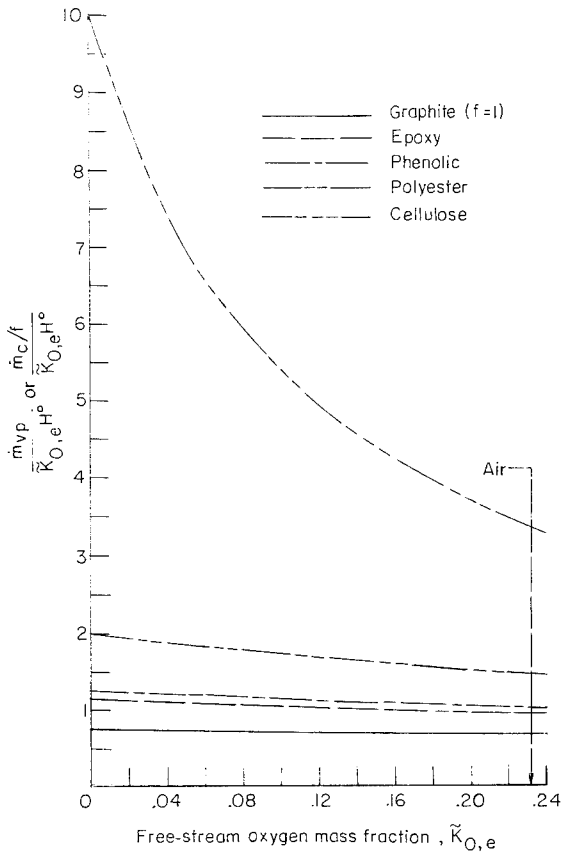

Figure 6.- Effect of virgin plastic composition on the ratio of ablation rate (or char oxidation rate) to diffusion oxygen flux.

Estimates of the weight of material ablated by a given aerodynamic heat load can be obtained by defining an "effective heat of ablation." For present purposes a cold-wall effective heat of ablation is used and is defined as follows:

$$Q_{eff} = \frac{q_{cw}^{\circ}}{\dot{m}_{vp}} = \frac{h^{\circ}H_s}{\dot{m}_{vp}} \tag{140}$$

Substitution of equation (139) into equation (140) yields

$$Q_{eff} = \left(\frac{fW^*}{\tilde{K}_{O,e}} + \eta \right) H_s \tag{141}$$

For diffusion-controlled oxidation, the response of the ablator is determined by the flux of oxygen to the char surface and is completely independent of the aerodynamic heat flux. As a result, equation (141) contains no thermal properties such as specific heats, thermal conductivities, or heats of pyrolysis. It is only in mass transport controlled cases, such as the present one, that an effective heat of ablation such as that defined in equation (140) has meaning. Where the response of the ablator is determined by aerodynamic heat flux, a thermochemical heat of ablation such as

$$Q^* = \frac{q_{net}}{\dot{m}_{vp}} \tag{142}$$

(where q_{net} is the heat flux to a nonablating calorimeter that has the same temperature, emissivity, and catalytic efficiency as the ablator) must be used.

Equation (141) was used to calculate values of Q_{eff} for each of the materials appearing in table I for $K_{O,e} = 0.232$, which corresponds to air. The variation of these effective heats of ablation with stagnation enthalpy is presented in figure 7, which shows

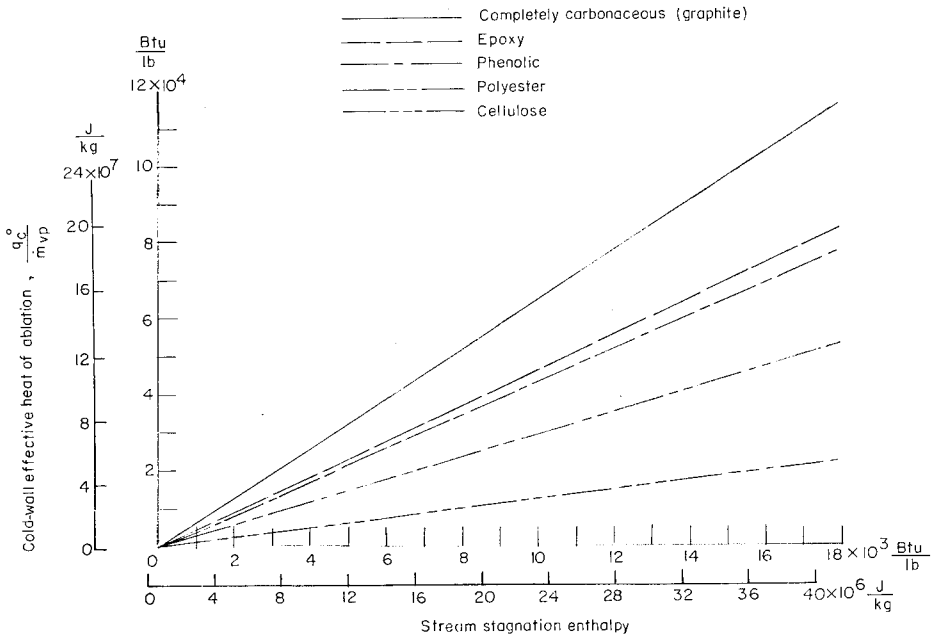

Figure 7.- Effect of virgin plastic composition on cold-wall effective heat of ablation.

that the cold-wall effective heats of ablation of epoxy, phenolic, polyester, and cellulose are, respectively, 72, 67, 45, and 19 percent of that for a completely carbonaceous material. Since, for a given cold-wall heat load, the weight of material ablated is inversely proportional to H_{eff}, figure 7 may be interpreted as showing that the respective weights of material ablated from heat shields composed of epoxy, phenolic, polyester, and cellulose would be 1.39, 1.49, 2.22, and 5.25 times the weight of material ablated from a completely carbonaceous shield.

Effect of Pyrolysis Gas Composition on the Heat Release Due to Chemical Reaction

In order to illustrate the effects of varying pyrolysis gas composition, calculations were made for two assumed pyrolysis gas compositions. These compositions, which are presented in table II, were based on data presented in references 13 and 14. The results

TABLE II

ASSUMED PYROLYSIS GAS COMPOSITIONS

Item	Composition 1 (phenolic resin)	Composition 2 (phenolic nylon)
$\bar{X}_{H_2}$	0.5199	0.2061
$\bar{X}_{CO}$	0.1954	0.2875
$\bar{X}_{N_2}$	0.0013	0
$\bar{X}_{CO_2}$	0	0.0222
$\bar{X}_{CH_4}$	0.1427	0.1980
$\bar{X}_{C_2H_2}$	0	0.1340
$\bar{X}_{C_2H_4}$	0	0.0006
$\bar{X}_{NH_3}$	0.1407	0.1515
$\bar{X}_{H_2O}$	0	0
fW^*	0.724	0.601
m_H	0.0974	0.0795
η	0.921	0.886
$C_\sigma H_\tau N_\nu O_\varphi$	$C_{5.9}\ H_{10.37}\ N_{0.73}\ O_1$	$C_{3.74}\ H_{5.80}\ N_{0.46}\ O_1$
f	0.462	0.23

of these calculations are compared with those for graphite and are presented in figures 8, 9, and 10.

From table II it is seen that the two compositions differ significantly with respect to H_2, CO, and C_2H_2 content. A comparison of table II with table I shows that the values of fW^* and the virgin plastic carbon and oxygen contents derived from the pyrolysis gas compositions are lower than those derived from the molecular structure of phenolic resin. Because of the extreme difficulty of experimentally determining pyrolysis gas composition, and because, in the compositions presented in table II trace species and condensibles included in references 13 and 14 were neglected, the compositions presented in table II must be considered as assumed rather than experimentally measured. Considered in this light, the agreement in fW^* is perhaps not too bad.

Figure 8 presents the boundary-layer composition at char surface as a function of $\tilde{K}_{O,e}$ for two assumed compositions and graphite. Comparing figure 8 with figure 5 shows that the char surface boundary-layer composition produced by the assumed pyrolysis gases closely approximates that derived from the molecular structure of phenolic resin.

In figure 9 the variation of the maximum heat of reaction (per pound of char) with char surface-temperature is presented for graphite and the two pyrolysis gas compositions. The maximum heat of reaction ΔH_R for composition 1 is only slightly lower than that for graphite, whereas ΔH_R for composition 2 is approximately twice that for graphite. A large part of this difference is due to the difference in f (mass of char produced when a unit mass of virgin material is pyrolyzed) between compositions 1 and 2. (See eq. (116).) Figure 9 shows that ΔH_R (per pound of char) can be a strong function of virgin plastic composition and pyrolysis gas composition.

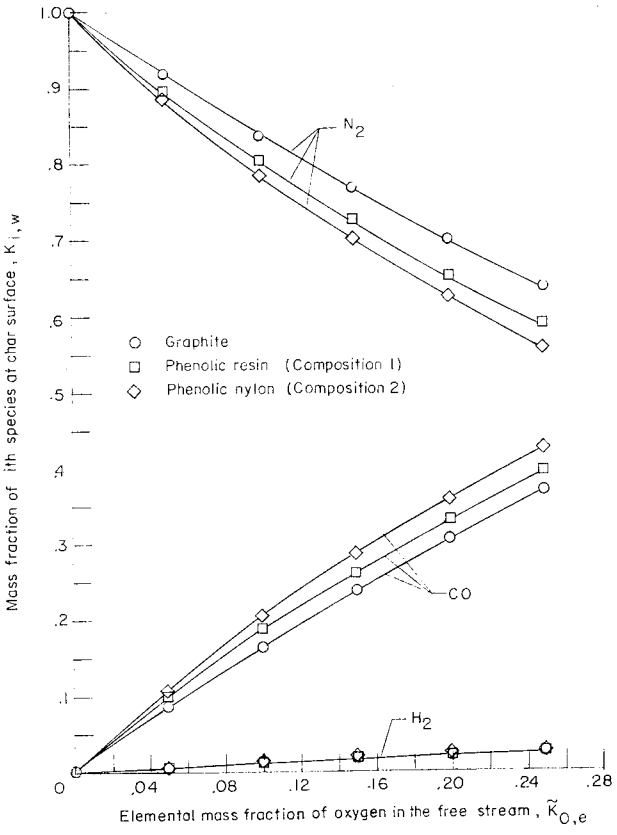

Figure 8.- Variation of boundary-layer composition at char surface with free-stream oxygen mass fraction as calculated from assumed pyrolysis gas compositions.

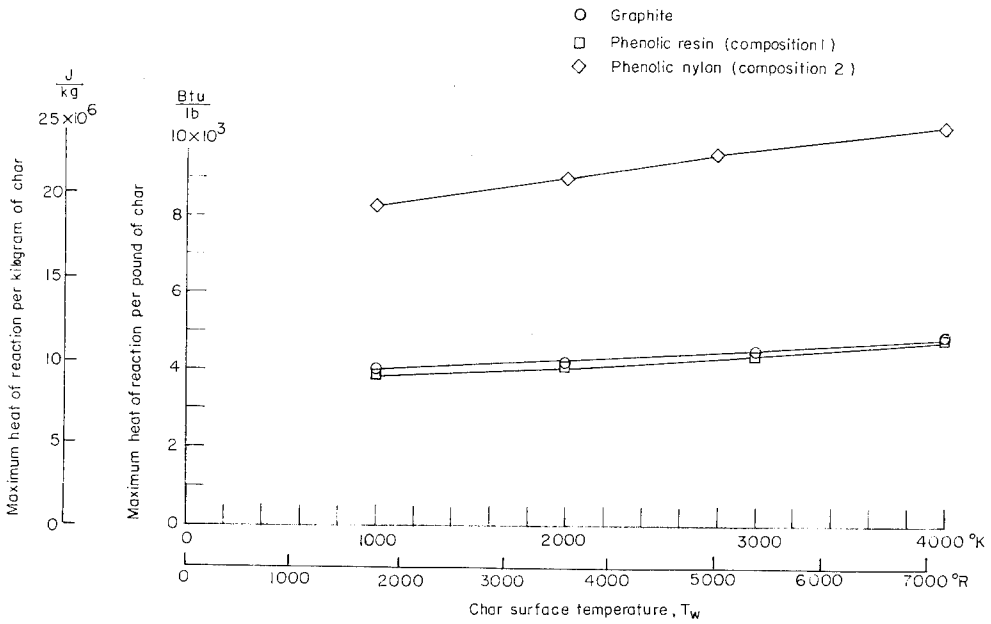

Figure 9.- Variation of maximum heat of reaction with char surface temperature as calculated from assumed pyrolysis gas compositions.

As shown by equations (117), (118), (119), and (134) an effective enthalpy potential due to chemical reaction can be defined as a function of virgin plastic composition, pyrolysis gas composition, and free-stream oxygen mass fraction. This effective enthalpy potential $\left(\text{per unit } \tilde{K}_{O,e}\right)$ is plotted against char surface temperature in figure 10. Note

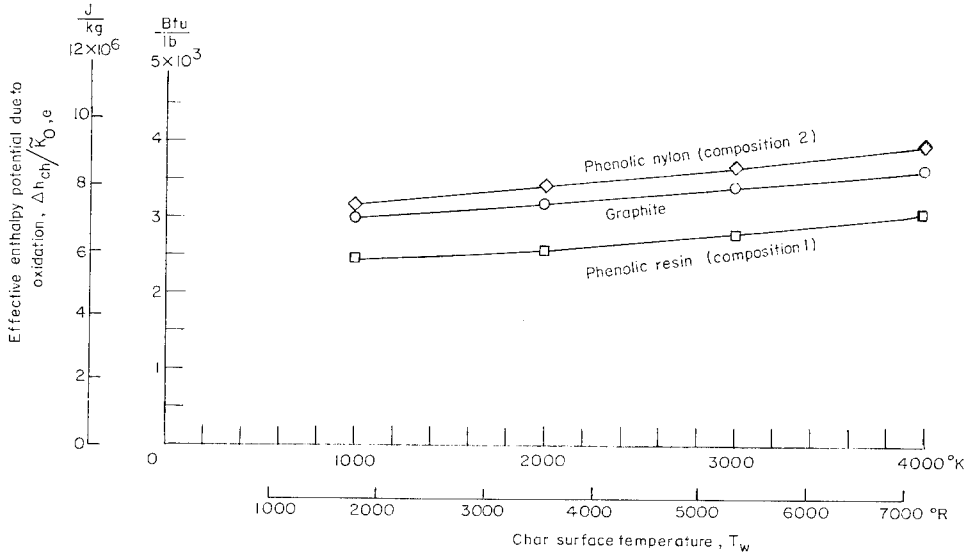

Figure 10.- Variation of effective enthalpy potential due to oxidation with char surface temperature as calculated from assumed pyrolysis gas compositions.

that ΔH_{ch} for composition 2 is larger than that for graphite whereas ΔH_{ch} for composition 1 is less than that for graphite. The parameters responsible for these differences can be identified by examining equation (134). Rearrangement of equation (134) yields

$$\Delta H_{ch} = \left(\Delta H_{ch}\right)_{C(s)} - \frac{\tilde{K}_{O,e}}{M_O}\left(\frac{\varphi}{\sigma - \varphi}\right)\left(\Delta H_{f,CO} - \frac{\sum_i \bar{X}_i \Delta H_{f,i}}{\bar{X}_{CO} + 2\bar{X}_{CO_2} + \bar{X}_{H_2O}}\right) \tag{143}$$

where the first term on the right-hand side is the effective enthalpy potential for the combustion of graphite. Note that the second term on the right-hand side will be positive or negative (and hence ΔH_{ch} will be greater than or less than $\left(\Delta H_{ch}\right)_{C(s)}$) depending on whether $\Delta H_{f,CO}$ is greater than or less than $\dfrac{\sum_i \bar{X}_i \Delta H_{f,i}}{\bar{X}_{CO} + 2\bar{X}_{CO_2} + \bar{X}_{H_2O}}$. Also note that for a given value of $\Delta H_{f,CO} - \dfrac{\sum_i \bar{X}_i \Delta H_{f,i}}{\bar{X}_{CO} + 2\bar{X}_{CO_2} + \bar{X}_{H_2O}}$ the magnitude of ΔH_{ch} depends on the size of the ratio $\left(\dfrac{\varphi}{\sigma - \varphi}\right)$. Since $\Delta H_{f,CO}$ is a negative quantity, ΔH_{ch} will be larger than $\left(\Delta H_{ch}\right)_{C(s)}$ when $\sum \bar{X}_i \Delta H_{f,i}$ is positive. Of all the pyrolysis gas constituents considered in this paper, only C_2H_2 and C_2H_4 have positive values of ΔH. Hence ΔH_{ch} becomes larger as the amounts of C_2H_2 and C_2H_4 in the pyrolysis gases increase. Note from figure 10 and table II that ΔH_{ch} for pyrolysis gas composition 2 (which contains C_2H_2) is larger than ΔH_{ch} for pyrolysis gas composition 1 (which does not contain C_2H_2). Vojvodich and Pope reported in reference 17 heating due to chemical reactions much larger than could be accounted for by carbon combustion. From equation (143) it is seen that very large values of ΔH_{ch} could be produced by a plastic which had a small value of $(\sigma - \varphi)$ and produced pyrolysis gases containing large amounts of C_2H_2 and C_2H_4.

SUMMARY OF RESULTS

An analytical study of diffusion-controlled char oxidation and its effect on the ablation of hydrocarbon plastics has been carried out. Although the solution obtained is based on a number of simplifying assumptions, it is believed to present an accurate conceptual picture of the diffusion-controlled char-oxidation process. The steady-state expressions resulting from this analysis can be used directly to provide a clear physical picture of char oxidation. This analysis has also produced general expressions which can be used in conjunction with a transient heat conduction computer program to yield transient ablation and char oxidation rates, but such a procedure does not lend itself to demonstrating the general characteristics of diffusion-controlled char oxidation. Accordingly, the discussion and results presented in the present report were restricted to the steady-state case. The results of this study are summarized as follows:

1. The present analysis differed from previous analyses of diffusion-controlled char oxidation in one important respect: previous investigators have assumed that only the carbon in the char layer would react and that the rate of reaction would be determined by the diffusion rate of oxygen through the boundary layer but the present analysis has shown that the carbon present in both the char and the pyrolysis gases (i.e., all the carbon originally present in the virgin plastic) reacts and that the reaction rate is determined by the rate at which oxygen can be supplied by diffusion through the boundary layer plus pyrolysis of the virgin plastic. Because of this fact, the char oxidation rate, the steady-state ablation rate, the boundary-layer composition at the char surface, and the heat released by chemical reactions were found to be dependent on the composition of the virgin plastic and the pyrolysis gases.

2. For a given flow environment (i.e., oxygen mass fraction and heat-transfer coefficient) the char oxidation rate and the pyrolysis rate were found to increase as the hydrogen, nitrogen, and oxygen contents of the virgin plastic increased and to decrease as the carbon content of the virgin plastic increased. Even when transpiration cooling effects were accounted for, the lowest steady-state pyrolysis rate was obtained from a material composed entirely of carbon.

3. The cold-wall effective heat of ablation of a plastic material was found to be determined by the free-stream oxygen mass fraction, the stream enthalpy potential, and relative number of carbon, hydrogen, nitrogen, and oxygen atoms in the virgin plastic. Example calculations carried out for a completely carbonaceous material, epoxy, phenolic and polyester resins, and cellulose showed that the effective heats of ablation for the polymers would be, respectively, 72, 67, 45, and 19 percent of the effective heat of ablation calculated for the carbonaceous material.

4. The maximum heat of reaction per pound of char was a strong function of pyrolysis gas composition and the fraction of virgin material which was converted to gas, and the heat released by both gas phase and heterogeneous reactions can be accounted for by an "effective enthalpy potential" which is a function of the stream oxygen mass fraction, the relative number of carbon, oxygen, hydrogen, and nitrogen atoms in the virgin plastic and the composition of the pyrolysis gases. The pyrolysis gases considered in this investigation were CO, CO_2, H_2, N_2, NH_3, H_2O, CH_4, C_2H_2, and C_2H_4. Both the maximum heat of reaction and the effective enthalpy potential were found to increase with increasing C_2H_2 and C_2H_4 content. Particularly high heat releases were predicted for polymers which contained nearly equal numbers of carbon and oxygen atoms and produced pyrolysis gases containing large quantities of C_2H_2 and and C_2H_4.

Langley Research Center,
National Aeronautics and Space Administration,
Langley Station, Hampton, Va., February 18, 1966.

REFERENCES

1. Scala, Sinclaire M.: The Ablation of Graphite in Dissociated Air. Part I: Theory. R62SD72, Missile and Space Div., Gen. Elec. Co., Sept. 1962.

2. Moore, Jeffrey A.; and Zlotnick, Martin: Combustion of Carbon in an Air Stream. ARS J., vol. 31, no. 10, Oct. 1961, pp. 1388-1397.

3. Denison, M. R.; and Dooley, D. A.: Combustion in the Laminar Boundary Layer of Chemically Active Sublimating Surfaces. J. Aeron. Sci. (Readers' Forum), vol. 25, no. 4, Apr. 1958, pp. 271-272.

4. Scala, S. M.; and Gilbert, L. M.: Aerothermochemical Behavior of Graphite at Elevated Temperatures. R63SD89, Missile and Space Div., Gen. Elec. Co., Nov. 1963.

5. Scala, S. M.; and Gilbert, L. M.: The Sublimation of Graphite at Hypersonic Speeds. R64SD55 (Contracts No. 04(647)-269 and AF 04(694)-222), Missile and Space Div., Gen. Elec. Co., Aug. 1964.

6. Mechtly, E. A.: The International System of Units - Physical Constants and Conversion Factors. NASA SP-7012, 1964.

7. Dow, Marvin B.; and Swann, Robert T.: Determination of Effects of Oxidation on Performance of Charring Ablators. NASA TR R-196, 1964.

8. Swann, Robert T.: Approximate Analysis of the Performance of Char-Forming Ablators. NASA TR R-195, 1964.

9. Lees, Lester: Convective Heat Transfer With Mass Addition and Chemical Reactions. Combustion and Propulsion - Third AGARD Colloquium, M. W. Thring, O. Lutz, J. Fabri, and A. H. Lefebvre, eds., Pergamon Press, 1958, pp. 451-498.

10. Fleddermann, Richard G.: Heat Transfer to a Vaporizing, Ablating Surface. J. Aero/Space Sci. (Readers' Forum), vol. 26, no. 9, Sept. 1959, pp. 604-605.

11. Swann, Robert T.; and Pittman, Claud M.: Numerical Analysis of the Transient Response of Advanced Thermal Protection Systems for Atmospheric Entry. NASA TN D-1370, 1962.

12. Fay, J. A.; and Riddell, F. R.: Theory of Stagnation Point Heat Transfer in Dissociated Air. J. Aeron. Sci., vol. 25, no. 2, Feb. 1958, pp. 73-85, 121.

13. Friedman, Henry L.: The Pyrolysis of Plastics in a High Vacuum Arc Image Furnace. T.I.S. Rept. R60SD380 (Contract NO. AF 04(647)269), Missile and Space Vehicle Dept., Gen. Elec. Co., May 1960.

14. Res. and Advanced Develop. Div., AVCO Corp.: Kinetics of Plastic Decomposition. AFSWC-TDR-62-102, U.S. Air Force, Sept. 1962. (Available from ASTIA as 332922.)

15. Kratsch, K. M.; Hearne, L. F.; and McChesney, H. R.: Thermal Performance of Heat Shield Composites During Planetary Entry. Presented at AIAA-NASA National Meeting (Palo Alto, Calif.), Sept. 30 - Oct. 1, 1963.

16. Anon.: JANAF Thermochemical Tables. Contract No. AF33(616)-6149, Thermal Lab., The Dow Chem. Co., June 30, 1962.

17. Vojvodich, Nick S.; and Pope, Ronald B.: Effect of Gas Composition on the Ablation Behavior of a Charring Material. AIAA J., vol. 2, no. 3, Mar. 1964, pp. 536-542.